

Photoemission from ordered thin films of Cu on Ni(100)

V. Rogge* and H. Neddermeyer†

*Institut für Experimentalphysik der Ruhr-Universität Bochum, Postfach 10 21 48,
D-4630 Bochum 1, Federal Republic of Germany*

(Received 8 December 1988; revised manuscript received 27 April 1989)

We have measured angle-resolved photoemission for Cu films on Ni(100) in the 0.4–12-monolayer coverage range. The growth of the films has been controlled by low-energy electron diffraction, Auger-electron spectroscopy, and ion-scattering spectroscopy. In the low-coverage range (≤ 4 monolayers) we observed two-dimensional dispersion of the Cu states; bulklike behavior was found for higher coverages. The transitions showed a systematic shift with increasing coverage to larger binding energies. No quantum size effects due to the discrete number of Cu layers could be detected.

I. INTRODUCTION

For an ordered layer-by-layer growth of a metal film on a metallic substrate the lattice mismatch $f = (a_m - a_s)/a_s$ (a_m and a_s being the lattice parameters of the overlayer material in its bulk form and of the substrate, respectively) must be as small as possible. Several authors have shown that thin films of Cu on Ag(001) grow epitaxially up to a coverage (Θ) of at most 2–3 monolayers (ML),^{1,2} because of a fairly large value of f [-0.12 (Ref. 3)] in this case. Using Ni(100) as the substrate the lattice mismatch is much smaller [$f = 0.026$ (Ref. 3)], which means that epitaxial growth of Cu on Ni(100) should continue up to larger values of Θ than for a Ag substrate. The use of a Ni(100) substrate would therefore open the possibility of studying the development of the electronic structure, with increasing Θ extending into the limit of bulklike behavior of the overlayer.

A number of experimental and theoretical investigations of the Cu/Ni(100) system have been reported. Chambers and Jackson found by using electron microscopy⁴ that at room temperature Cu grows pseudomorphic on Ni(100) up to $\Theta = 4$ ML. In this range the average lattice parameter of the overlayers gradually changes from that of the substrate to that of bulk Cu. This is only possible if elastic strain is incorporated in the atomic layers of Cu. As a consequence, the system follows only approximately the ideal layer-by-layer growth mode. In Ref. 4 the term “uneven layer growth” has been used for characterizing the growth process. In a more recent low-energy-electron transmission experiment, Iwasaki *et al.* observed pseudomorphic growth up to $\Theta = 6$ ML and characteristic quantum-size effects for thin films.⁵ The latter phenomena is of interest for the electronic states of the deposited Cu film, which could be quantized with the number of atomic layers.⁶ In photoemission the quantization should give rise to splitting of individual transitions. A direct and convincing photoemission observation of the quantum-size effect in a film structure has not yet come to our attention.

In the present work the electronic structure of

Cu/Ni(100) has been investigated by means of angle-resolved ultraviolet photoemission spectroscopy (ARUPS). The growth mode of the Cu overlayers in the range of $0.4 \leq \Theta \leq 12$ ML was examined with Auger-electron spectroscopy (AES), ion-scattering spectroscopy (ISS), ARUPS, and low-energy electron diffraction (LEED). While the AES and ARUPS data may be explained by the layer-by-layer growth mode, ISS clearly showed that under the chosen temperature conditions of the Ni substrate (room temperature during Cu deposition with subsequent annealing to 520 K) the system does not follow *exactly* this type of growth mode. For example, the second atomic Cu layer already starts growing when the first layer has covered only about 85% of the sample surface. This effect leads to deviations from the ideal growth mode in the form of a small atomic roughness of the Cu film. LEED pattern and ARUPS results for small coverage ($0.4 \leq \Theta \leq 4$ ML) are not sensitive enough to detect these small deviations from ideal growth behavior. They may fully be explained by the assumption of essentially well-ordered epitaxial growth. Due to insufficient accuracy of the refraction-data effects as splitting of beams or a gradual change of beam positions with increasing coverage due to the lattice mismatch could not be detected.

For $\Theta = 1$ ML the Cu d states showed two-dimensional dispersion, in agreement with theoretical results for a Cu/Ni(100)/Cu sandwich computed by Zhu *et al.*⁷ if a rigid shift of the calculated binding energies is taken into account. With increasing number of overlayers the two-dimensional energy bands systematically shift to larger binding energies. A splitting of transitions corresponding to the number of atomic layers due to a quantum-size effect could not be observed. Bulklike behavior of Cu transitions was found for $\Theta \geq 4$ ML. The 12 ML Cu overlayer exhibits the same d -like surface state, which is characteristic of bulk Cu(100).⁸

A brief discussion of experimental details including the analysis of the film structure is given in Sec. II. Our ARUPS results are presented in Sec. III and are compared and discussed in the light of other work in Sec. IV. Concluding remarks are given in Sec. V.

II. EXPERIMENT

The experimental equipment consists of a spectrometer and a preparation chamber, which are connected via a gate valve. A modified ESCA 3 electron spectrometer (Vacuum Generators) is employed as energy analyzer. The original slit system has been modified to allow angle-resolved measurements. The energy and angular resolutions are $\Delta E/E = 0.012$ (full width at half maximum) and $\Delta\alpha = \pm 3.6^\circ$ (full opening, for the ARUPS measurements), respectively. For ARUPS the samples are irradiated with unpolarized noble-gas resonance radiation and for ISS with Ne or He ions (normally 1.5 keV), which are produced by a MINIBEAM I ion gun (Kratos). By changing the polarity of the acceleration voltage, the same gun may be utilized as electron source for excitation of the Auger electrons. The angle between incident radiation and emission is always constant.

The Ni(100) substrate was treated in the preparation chamber with numerous cycles of Ar^+ (450 eV) bombardment and heating (700 K). As final surface contamination, traces of C (by means of AES) and O (using ISS) were visible with intensity close to the detection limit of our analytical methods. The LEED pattern of Ni(100) showed the expected integral-order and weak half-order spots, the latter being possibly associated with the incorporation of some C atoms in the uppermost atomic layer.⁹ A water-cooled effusion cell with integral quartz microbalance has been developed for evaporation of the Cu atoms. The films were deposited on the room-temperature Ni substrate with subsequent annealing at 520 K, which produced a sharpening of the Cu-related structures in the energy distribution curves (EDC's) of the photoemitted electrons. In LEED the weak half-order spots of the "clean" substrate disappeared with increasing Θ . Sharp integral-order beams indicated the existence of long-range order in the overlayer structures. A more quantitative analysis of the refraction data was not attempted. Qualitatively, we did not observe broadening or splitting of beams due to the differences in the Cu and Ni lattice parameter, nor did we observe distinct shifts of beam positions with increasing coverage. ISS spectra recorded with maximum sensitivity to surface contamination showed the presence of some B, C, and O, whose concentration was estimated to be smaller by 2 orders of magnitude compared to those of the metal atoms.

The general characteristics of the film growth were derived from the AES intensities of the Cu L_3VV (920 eV) and Ni $L_3M_{2,3}M_{2,3}$ transitions [Fig. 1(a)] and the ARUPS intensity ratio of Cu and Ni $3d$ normal-emission peaks as a function of coverage [Fig. 1(b)]. The AES results are consistent with the layer-by-layer growth mode leading to an exponential dependency of the intensities and a mean free path of the Auger electrons of 0.83 nm.¹⁰ Completion of atomic layers is usually recognized by the occurrence of breakpoints in the intensity curves. Such breakpoints are not visible in our results due to insufficient number of data points and probably (see ISS results below) due to small differences between actual and ideal growth modes.

In the case of layer-by-layer growth, and neglecting

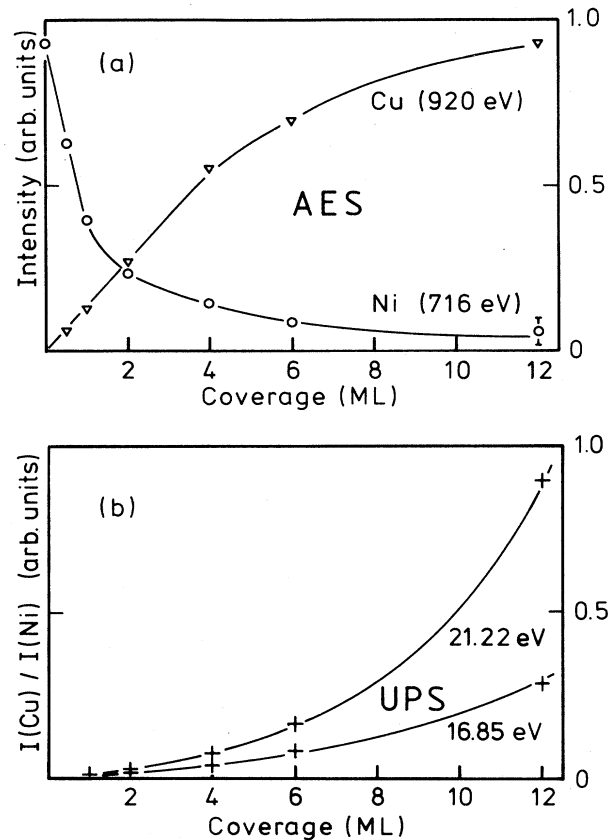


FIG. 1. (a) Auger-electron-spectroscopy (AES) intensities as a function of Cu coverage obtained under constant operation conditions of the electron gun. (b) Photoemission intensity ratio $I_{\text{Cu}}/I_{\text{Ni}}$ as a function of Cu coverage.

atomic roughness, the ARUPS intensity ratio $I_{\text{Cu}}/I_{\text{Ni}}$ should be proportional to $\exp(d/\lambda) - 1$, where d is the overlayer thickness and λ the mean free path of $3d$ photoelectrons from Cu and Ni, which is assumed here to be only dependent on the photon energy. Fitting the experimental data [Fig. 1(b)], we obtained $\lambda_{21.22 \text{ eV}} = 0.74 \pm 0.04$ nm and $\lambda_{16.85 \text{ eV}} = 1.04 \pm 0.04$ nm, which is in good agreement with the "universal" mean-free-path curve of electrons in solids.¹¹

By using Ne in the ISS gun the Cu surface concentration can be determined quantitatively.¹² As discussed more thoroughly in Ref. 12, the procedure to obtain concentration values for the uppermost atomic layer is complicated by the sputtering effect, which leads to a change of the actual surface concentration during the ISS measurements, and an intermixing of atomic layers in the surface region within a typical depth of 1 nm. The initial surface concentration of the Cu and Ni components can be obtained by time-dependent measurements assuming a constant ion current and extrapolation to $t = 0$. In Fig. 2 we show the results of such an experiment, where the intensity of the Cu peak in the ISS data in relation to that of the Ni peak is plotted against the irradiation dose. The irradiation dose should be proportional to the num-

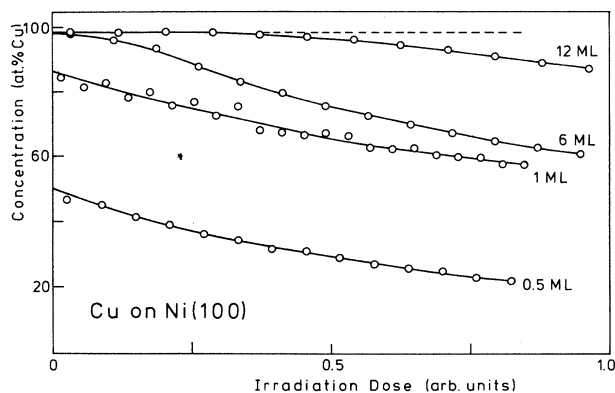


FIG. 2. Ion-scattering-spectroscopy (ISS) data from the system Cu on Ni(100) by using Ne ions of 1.5 keV energy. The spectra used for evaluation of the data points are collected in typically 1 min.

number of ions impinging on the sample surface. This quantity, which as a matter of fact is directly proportional to t , has been chosen as abscissa, since the gas pressure used for bombardment was individually adjusted for measurement of the various overlayers. The dependency of the irradiation dose as a function of gas pressure has been determined in a previous experiment.¹³ We note that the ion current was not measured routinely during the measurements. A typical value for the current density was 3 nA/mm².

It has been shown in Ref. 12 that ISS detects Cu and Ni atoms with the same efficiency, which means that the ratio of the peak intensities is a measure of the relative concentration of both components. As expected, the 6 and 12 ML Cu films display 100% Cu concentration at the beginning of the ISS measurements. For the 6-ML structure Ni becomes visible almost immediately after beginning of the irradiation, which we explain by an intermixing of the constituents induced by the bombardment process. Along the same lines, the 12-ML overlayers require a larger dose for the combined effects of intermixing and removal of Cu surface atoms to yield a detectable decrease of the Cu signal. For 0.5 ML of Cu the initial Cu surface concentration (obtained by extrapolating the data points to an irradiation dose of 0) is 50%, while the 1-ML film reaches only 85%. This may be explained by an incomplete coverage of the substrate surface for a nominal deposition of 1 ML and a beginning growth of the second atomic Cu layer prior to completion of the first one. The ARUPS spectra of the 1 ML Cu film will therefore contain some contribution from the 2-ML structure and the possibility of an atomic roughness has to be kept in mind for interpretation of the data.

In summary, the exponential dependence of AES and ARUPS results may be explained essentially by the layer-by-layer growth mode of the Cu overlayer. ISS data and possibly absence of breakpoints in the AES intensities indicate, however, that small deviations from ideal growth characteristics exist.

III. RESULTS

EDC's from a Cu monolayer on Ni(100) are displayed in Fig. 3 as a function of the polar emission angle ϑ in the $\Gamma K W X$ plane of the Brillouin zone. The Cu-induced transitions (marked by vertical bars) are found in the energy range between -4.5 and -1.5 eV and correspond to the Cu d states. The energy range up to the Fermi level E_F reflects the Ni d states and does not show noticeable differences (except for their intensity) relative to those of the clean substrate, which for $\vartheta=0$ is shown as a dashed line.¹⁴ In normal emission only one Cu transition is seen, which in the off-normal direction splits into various components. We note that even at $\Theta=0.4$ ML the Cu-related transitions (with reduced intensity) exhibited a similar dispersion as the 1-ML film, which we interpret by a tendency of the Cu deposit to grow in form of two-dimensional islands. It should be mentioned that in the submonolayer range we never observed emission comparable to that of the free Cu atoms, which should give rise to four separate peaks corresponding to the final-state configurations 1D_2 , 3D_1 , 3D_2 , and 3D_3 .¹⁵ We did not at-

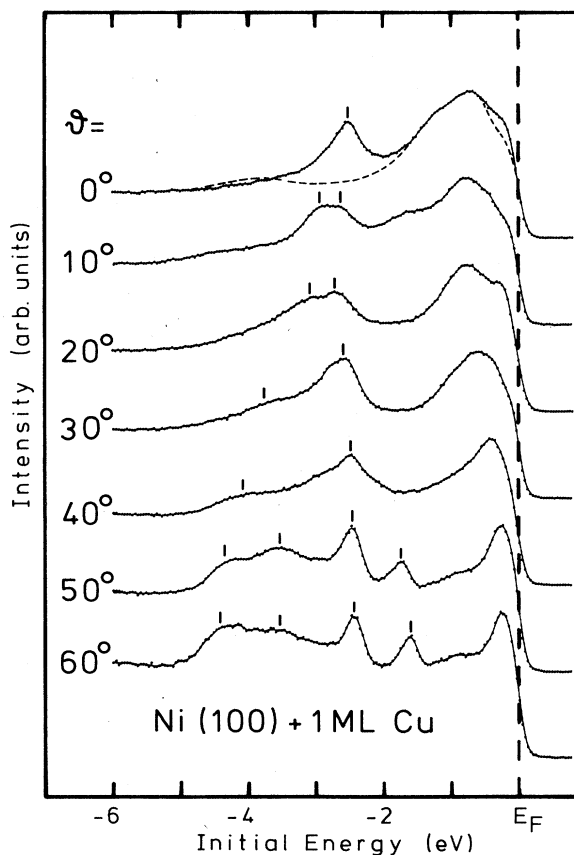


FIG. 3. EDC's from 1 monolayer (ML) of Cu on Ni(100) measured as a function of polar angle of emission ϑ in the $\Gamma K W X$ plane of the bulk Brillouin zone. The photon energy was 21.22 eV. The Cu-related transitions are marked with a vertical bar. Normal emission from Ni(100) is shown as a dashed line.

tempt to use angular ISS scans of the sample for a more quantitative analysis of surface geometry. Two-dimensional clustering in the submonolayer range can therefore not be identified in our ISS results.

The peak positions in the EDC's of Fig. 3, together with the corresponding results for a 2 ML and 4 ML Cu film, are collected in a structure plot in Fig. 4. The most striking phenomenon is the obvious difference in peak position for every overlayer structure. A closer inspection shows that with increasing Θ the positions for the various films shift to lower initial energies but follow the same dispersion. A splitting of the features in the 2- and 4-ML films due to a quantum-size effect cannot be detected. More precisely, the splitting of bands corresponding to the number of monoatomic layers⁶ must be smaller (if it exists) than the measured width of the photoemission transitions. For $\Theta=4$ ML and small polar angle of emission ($<20^\circ$), transitions from the high-lying Cu *sp* band (labeled *a*) could be identified. The results of this particular film cannot be fully described in the two-dimensional Brillouin zone. The transition denoted "b" does not correspond to a transition of bulk Cu(100).

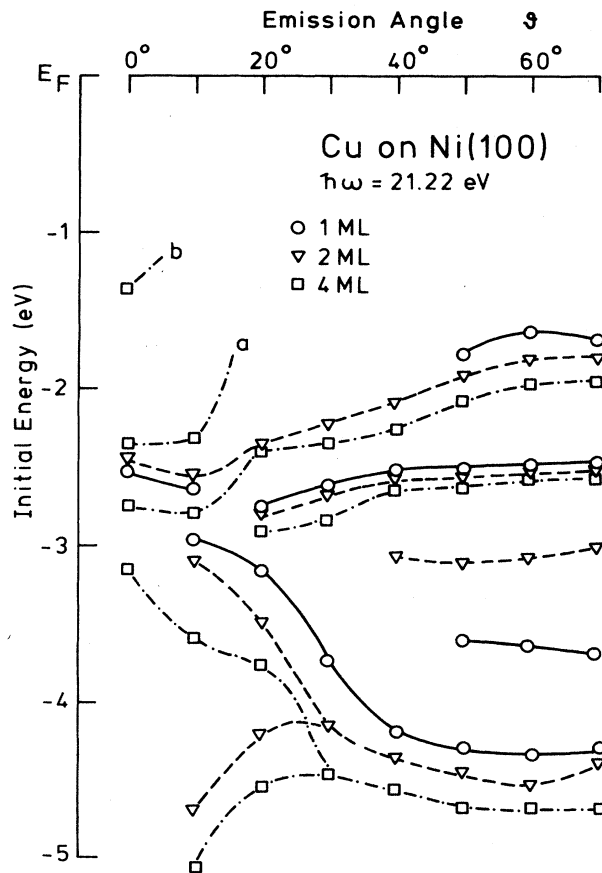


FIG. 4. Structure plot of Cu-related transitions in EDC's from Cu/Ni(100) for $\Theta=1$ ML (circles), 2 ML (triangles), and 4 ML (squares). The lines are a guide for the eye.

In Fig. 5 a comparison is made between the EDC's of a 12 ML Cu film and of bulk Cu(100).⁸ The latter results have been obtained by using a different instrument with superior energy and angular resolution, which may account for some differences in the observed width of the experimental structure. Deviations from ideal epitaxial growth may also contribute to the experimental width. For example, an atomic roughness of the Cu film may lead to scattering of the photoelectrons and therefore to additional contributions of neighboring directions of the photoemitted electrons resulting in a broadening of transitions. The dispersion of the peaks from the 12-ML film is in satisfactory agreement with that of bulk Cu, as is expected from an ordered epitaxial growth of the Cu deposit. The only difference in both sets of data is a small systematic shift by 0.08 eV of the overlayer peaks towards lower initial energies. At a polar angle of 60° , emission from the *d*-like surface state is recognized in the EDC of the evaporated Cu film as a shoulder (SS).

Two dimensionality of the Cu states for the 1- and 2-ML films has been confirmed by using different photon energies and by examining whether the measured disper-

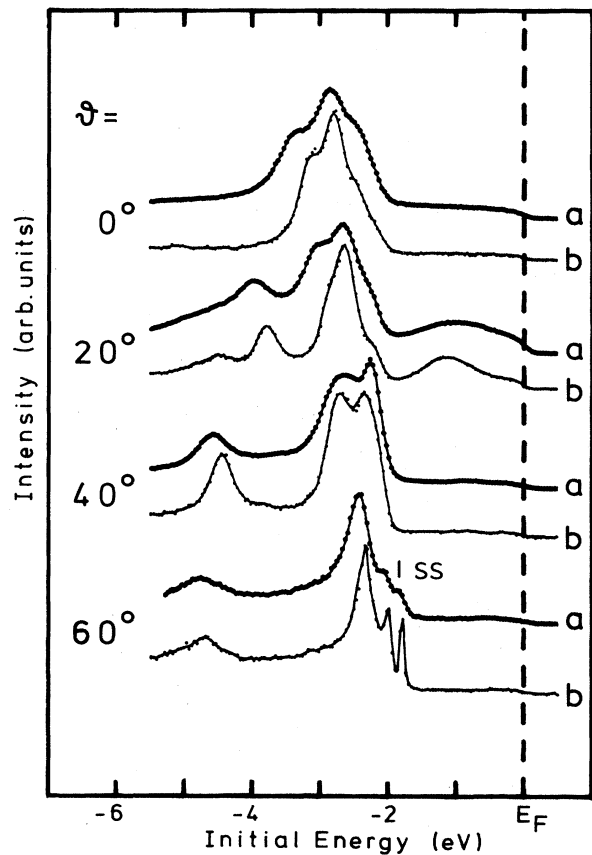


FIG. 5. Comparison of EDC's from 12 ML of Cu on Ni(100) (labeled *a*) with those of bulk Cu(100) (Ref. 8) (labeled *b*) for various polar angles of emission ϑ .

sion of the energy bands (Fig. 6) may be characterized by the parallel component of the wave vector (k_{\parallel}). We have computed k_{\parallel} in the usual way by the expression $k_{\parallel}(\text{\AA}^{-1}) = 0.5121(\hbar\omega + E_i - \Phi_w)^{1/2} \sin\vartheta$, where $\hbar\omega$ is the photon energy, E_i the initial energy, Φ_w the work function of the sample (all quantities measured in eV), and ϑ

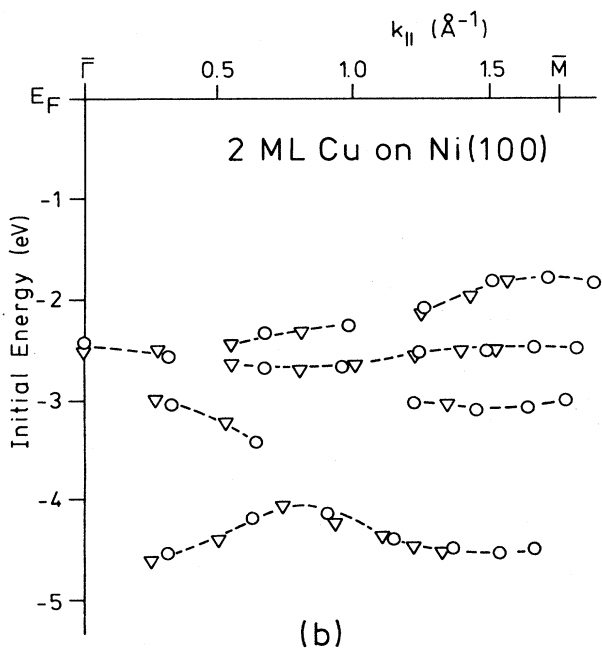
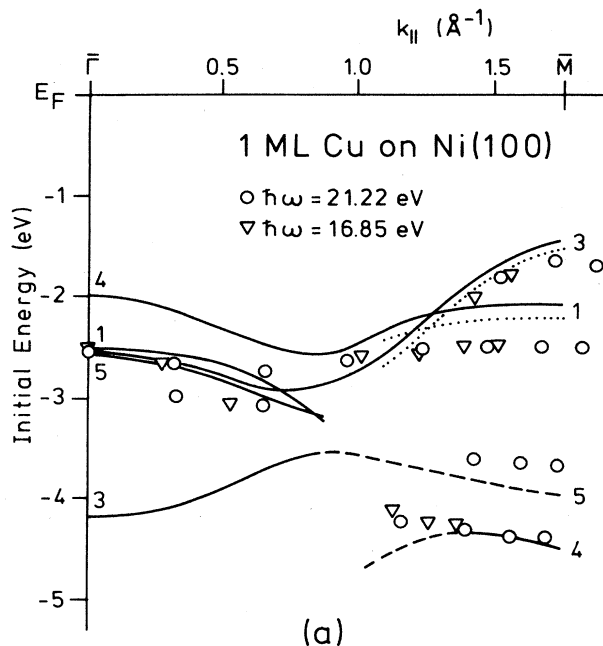


FIG. 6. (a) Two-dimensional dispersion of Cu-related transitions from 1 ML Cu on Ni(100) in comparison with theoretical energy bands of Ref. 7. (b) Two-dimensional dispersion from 2 ML Cu on Ni(100). The dashed lines are a guide for the eye.

the polar emission angle. The work function has been determined from the low-energy photoemission threshold. For clean Ni(100) we found $\Phi_w = 5.28 \pm 0.05$ eV and, for 12 ML Cu on Ni(100), $\Phi_w = 4.34 \pm 0.05$ eV. In Fig. 6(a) the results from 1 ML Cu on Ni(100) are plotted together with the Cu-derived portion of a theoretical energy-band structure of a Cu/Ni(100)/Cu sandwich, computed by Zhu *et al.* by means of a self-consistent local-orbital method.⁷ The theoretical energy bands [solid lines in Fig. 6(a)] are shifted downward by 0.6 eV in order to align the experimental normal-emission results with the theoretical data. The comparison is made with the theoretical minority-spin bands. The position of the majority-spin bands are indicated near \bar{M} by the dotted lines. The expected exchange splitting is too small to be resolved in our measurements. The solid lines correspond to states with at least 70% surface character; the dashed lines indicate states with 50–70% surface character. The agreement between experiment and theory is very satisfactory. The experimental splitting of the energy-band structure near \bar{M} into four components and their dispersion is well reproduced by the theory. The theoretical bands starting at $\bar{\Gamma}_4$ and $\bar{\Gamma}_3$ cannot be observed experimentally for small k_{\parallel} , since they are symmetry forbidden in normal emission.¹⁶ The 2-ML film [Fig. 6(b)] shows two-dimensional dispersion relations, which are very similar to the results from the 1-ML structure. One difference (in addition to the small energy shift, see Fig. 4) is the occurrence of an energy band at -3 eV near \bar{M} , which is absent for the 1-ML film and, for the 4-ML results, hardly recognizable by weak shoulders on the low-energy side of the main transitions.

Finally, the evolution of the energy position of the levels of X_5 and X_3 symmetry in the bulk band structure of Cu is shown in Fig. 7 as a function of Θ . Here we use the

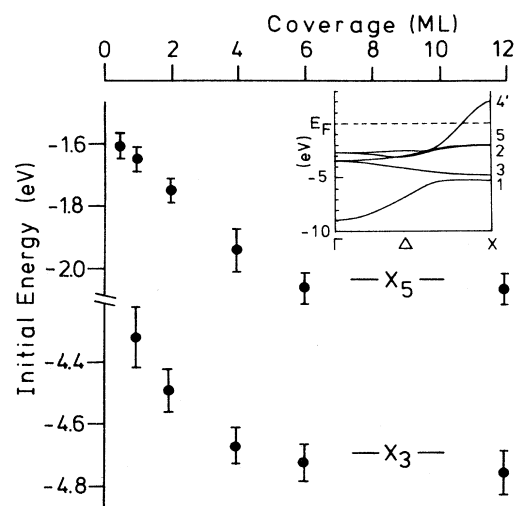


FIG. 7. Development of the energy position of the X_3 - and X_5 -symmetry points with Θ . The inset shows the band structure of Cu in the ΓX direction as calculated by Burdick (Ref. 17).

property that at a photon energy of 21.22 eV and a polar angle of emission at 60° one probes direct transitions near the X point of the bulk Brillouin zone. The same conditions lead to emission of two-dimensional features at \bar{M} in the two-dimensional Brillouin zone. In Fig. 7 we have plotted the position of the uppermost (ignoring feature SS of Fig. 5) and lowermost Cu-related transitions in the film spectra together with the results from bulk Cu(100) (Ref. 8) (horizontal bars). The systematic shift of the transitions with increasing coverage towards lower initial energies (maximum shift 0.4 eV) is apparent (also see Fig. 4). As has already been mentioned above, the transitions from the 12-ML structure are located distinctly below those of bulk Cu. A downward shift of peaks with increasing coverage has even been found in the submonolayer range. For example, in normal emission the Cu transition shifted by 0.05 eV upon increasing Θ from 0.4 to 0.5 ML. As deduced from the difference in the energy positions of the X_5 and X_3 levels, within the limits of experimental uncertainty no d band narrowing¹⁸ in the thin films compared to the d -band width of bulk Cu is seen.

IV. DISCUSSION

First, some details of the growth mode have to be discussed. A noticeable ISS observation was that for $\Theta=1$ ML the second atomic layer already starts growing before the substrate is covered completely. On the other hand, AES and ARUPS did not show a tendency to three-dimensional clustering, which is normally recognized by distinct deviations from exponential dependency of the intensities for large Θ . That such deviations are absent is an indication for only small differences to ideal behavior, which, in our opinion, may be described by an atomic roughness of the condensed overlayer. It is qualitatively clear that for formation of a complete atomic layer two-dimensional diffusion processes are necessary to transport the incoming Cu atoms to steps, kinks, or other high-binding-energy sites for condensation. If the surface is nearly covered with a monoatomic Cu layer, the impinging atoms may find high-binding-energy sites already atop the first (incomplete) layer, which would explain the ISS results. Further deposition would then lead to a completion of the first monolayer. The lattice mismatch of nearly 3% is probably too small to produce effects large enough to be seen with the applied experimental techniques. Two dimensionality of the ARUPS results for small Θ and a satisfactory agreement between the EDC's of the 12-ML film and of bulk Cu(100) are further manifestations for a nearly ideal layer-by-layer growth mode in the coverage range studied.

To our knowledge, the occupied electronic states of Cu on Ni(100) have not yet been studied experimentally. We note that an analogous band structure has been mapped for a $\text{Ni}_{0.84}\text{Cu}_{0.16}$ (111) surface, where an ordered monoatomic Cu layer can be produced by surface segregation.¹⁹ In Ref. 19 the dispersion of the Cu-related transitions from the alloy surface has been shown to be in close correspondence with the calculated energy bands of a free Cu(111) monolayer (except for their energy positions). In the present work the energy bands for the Cu monolayer

on Ni(100) are also well reproduced by theory⁷ if one takes into account a rigid shift of 0.6 eV of the theoretical bands towards lower energies.

Iwasaki *et al.*⁵ have derived values for the energy position of the X_1 point in the unoccupied part of the band structure for Ni(100) and for a thick Cu film on Ni(100). They assumed the position of X_1 to be constant for the various films, which is in contrast to our observation of a systematic shift of the occupied energy bands with increasing film thickness. Several possibilities have to be considered for an explanation of this effect. The main origin may result from a small charge transfer between overlayer and substrate, although in Ref. 7 such a phenomenon is not considered to be important. If, for example, some Cu valence charge is transferred to the Ni substrate, the reduction of screening of the Cu core potential may indeed lead to an increase of electronic binding energies for the Cu $3d$ states. It has to be noted that on the basis of the electronegativity scale [Ni, 1.8; Cu, 1.9 (Ref. 20)] the charge transfer cannot be large and should actually occur in the opposite direction. More theoretical work is needed to estimate the possible role of a charge transfer to explain the experimental shifts.

Another effect, which may influence the position of the energy bands, is the registration of the Cu overlayer relative to the Ni lattice for small Θ . Although the necessary lattice compression for Cu is quite small ($\approx 3\%$), it will cause small changes of the reciprocal lattice compared to that of bulk Cu and lead to a different position of E_F (depending on the occupation of available states), if we refer E_F to the low-energy band edge.

The influence of the Cu overlayers on the Ni d states, which in Ref. 7 and in previous theoretical work²¹ is predicted to lead to a reduction of the Ni magnetic moment at the interface and a change of the exchange splitting, could not be resolved in our experiment. A Ni(111) substrate would offer a better possibility to study such effects. For the latter surface in normal-emission results the exchange splitting could clearly be resolved in the vicinity of E_F ,²² which is hardly possible for Ni(100) because of too many overlapping energy bands. We note that we also did not find any clear evidence for a well-defined interface state between the Cu layers and the Ni substrate.

ARUPS studies on comparable systems have been reported for Cu on Ag(100) by Stoffel *et al.*² and for Cu(001)- $c(2\times 2)$ Pd by Wu *et al.*²³ The system Cu on Ag(100) shows behavior similar to Cu/Ni(100), at least in the low-coverage regime, when the above-mentioned lattice mismatch does not yet lead to an imperfect growth of the Cu films. One difference is seen in the normal-emission data, which exhibits a splitting of the Cu d transitions for the Ag substrate. A systematic shift of energy bands with the number of monolayers is not observed for Cu/Ag(100). In general, the analysis of the Cu/Ag(100) data is more difficult, because of considerable overlap between Ag and Cu transitions for small Θ , and large deviations from layer-by-layer-type growth of the Cu overlayers due to the differences in lattice mismatch. The d - d interaction between Cu and Ag electrons and charge transfer may also be different relative to the Cu/Ni case.

For Cu/Pd in Ref. 23, the results were interpreted as reflecting the formation of a surface alloy, which we rule out for Cu/Ni(100) on the basis of our ISS measurements.

V. CONCLUSION

We have measured Cu films on Ni(100) up to a coverage of 12 ML. Two-dimensional energy bands for the Cu films have been identified up to $\Theta=4$ ML. The experimental dispersion of the 1 ML Cu film is in good agreement with the Cu-derived states of a hypothetical Cu/Ni(100)/Cu sandwich as computed by Zhu *et al.*, provided a 0.6-eV shift of the theoretical energy bands towards lower energies is taken into account. Bulk transitions are found to some extent already at $\Theta=4$ ML and

are fully developed at $\Theta=12$ ML. The latter film shows distinct emission from a *d*-like surface state, which indicates ordered and epitaxial growth of the Cu overlayers. The experimental energy bands shift by 0.4 eV to lower initial energies with increasing number of layers and reach the bulk positions at approximately $\Theta=6$ ML. For the 12-ML film the observed *d*-electronic structure is lowered in energy by 0.08 eV compared to bulk Cu. The predicted splitting of the electronic levels (Ref. 6) due to quantum-size effects could not be detected.

ACKNOWLEDGMENTS

This work has been supported by the Deutsche Forschungsgemeinschaft (Bonn, Germany).

*Present address: Krupp-Pulvermetall, D-4300 Essen, Federal Republic of Germany.

[†]To whom correspondence should be addressed.

¹G. C. Smith, C. Norris, and C. Binns, *J. Phys. C* **17**, 4389 (1984).

²N. G. Stoffel, S. D. Kevan, and N. V. Smith, *Phys. Rev. B* **32**, 5038 (1985).

³C. Kittel, *Introduction to Solid State Physics*, 5th ed. (Wiley, New York, 1976).

⁴A. Chambers and D. C. Jackson, *Philos. Mag.* **31**, 1357 (1975); references to previous work may be found therein.

⁵H. Iwasaki, B. T. Jonker, and R. L. Park, *Phys. Rev. B* **32**, 643 (1985).

⁶P. D. Loly and J. B. Pendry, *J. Phys. C* **16**, 423 (1983).

⁷X.-Y. Zhu, H. Huang, and J. Hermanson, *Phys. Rev. B* **29**, 3009 (1984).

⁸P. Heimann, J. Hermanson, H. Miosga, and H. Neddermeyer, *Phys. Rev. B* **20**, 3059 (1979).

⁹J. H. Onuferko, D. P. Woodruff, and B. W. Holland, *Surf. Sci.* **87**, 357 (1979).

¹⁰M. P. Seah, *J. Phys. F* **3**, 1538 (1973).

¹¹I. Lindau and W. E. Spicer, *J. Electron. Spectrosc. Relat. Phenom.* **3**, 409 (1974).

¹²Th. Berghaus, Ch. Lunau, H. Neddermeyer, and V. Rogge, *Surf. Sci.* **182**, 13 (1987).

¹³Th. Berghaus, Diplomarbeit, Ruhr-Universität Bochum, Bo-

chum, Federal Republic of Germany, 1983.

¹⁴Results from uncovered Ni(100) are only shown for $\vartheta=0$, since a different state of surface conditions (cleanliness and morphology) for Ni(100) at the beginning of the experiment gave rise to a background in the Cu 3*d* region, which increased with ϑ and made a comparison of both data sets unreasonable.

¹⁵Photoemission from free Cu atoms is expected to show the same four components as those of free Ag atoms [M. O. Krause, *J. Chem. Phys.* **72**, 6474 (1980)].

¹⁶J. Hermanson (private communication).

¹⁷G. A. Burdick, *Phys. Rev.* **129**, 138 (1963).

¹⁸H. Krakauer, M. Posternak, and A. J. Freeman, *Phys. Rev. B* **19**, 1706 (1979).

¹⁹P. Heimann, J. Hermanson, H. Miosga, and H. Neddermeyer, *Solid State Commun.* **37**, 519 (1981).

²⁰L. Pauling, *The Nature of the Chemical Bond*, 3rd ed. (Cornell University Press, Ithaca, NY, 1960).

²¹J. Tersoff and L. M. Falicov, *Phys. Rev. B* **25**, 2959 (1982); **26**, 6186 (1982).

²²P. Heimann and H. Neddermeyer, *J. Phys. F* **6**, L257 (1976); D. E. Eastman, F. J. Himpsel, and J. A. Knapp, *Phys. Rev. Lett.* **40**, 1514 (1978).

²³S. C. Wu, S. H. Lu, Z. Q. Wang, C. K. C. Lok, J. Quinn, Y. S. Li, D. Tian, and F. Jona, *Phys. Rev. B* **38**, 5363 (1988).